DOI: 10.1534/genetics.108.092932

# Sequential Elimination of Major-Effect Contributors Identifies Additional Quantitative Trait Loci Conditioning High-Temperature Growth in Yeast

**Himanshu Sinha,*[,1,2] Lior David,[†,2] Renata C. Pascon,[‡] Sandra Clauder-Münster,* Sujatha Krishnakumar,[§] Michelle Nguyen,[§] Getao Shi,* Jed Dean,[§] Ronald W. Davis,[§] Peter J. Oefner,[§,**] John H. McCusker[‡] and Lars M. Steinmetz*[,§,3]**

**European Molecular Biology Laboratory, 69117 Heidelberg, Germany, [†]Department of Animal Sciences, Hebrew University of Jerusalem, Rehovot 76100, Israel, [‡]Department of Molecular Genetics and Microbiology, Duke University Medical Center, Durham, North Carolina 27710, [§]Stanford Genome Technology Center, Palo Alto, California 94304 and **Institute of Functional Genomics, University of Regensburg, 93053 Regensburg, Germany*

Manuscript received June 24, 2008
Accepted for publication August 1, 2008

ABSTRACT

Several quantitative trait loci (QTL) mapping strategies can successfully identify major-effect loci, but often have poor success detecting loci with minor effects, potentially due to the confounding effects of major loci, epistasis, and limited sample sizes. To overcome such difficulties, we used a targeted backcross mapping strategy that genetically eliminated the effect of a previously identified major QTL underlying high-temperature growth (Htg) in yeast. This strategy facilitated the mapping of three novel QTL contributing to Htg of a clinically derived yeast strain. One QTL, which is linked to the previously identified major-effect QTL, was dissected, and *NCS2* was identified as the causative gene. The interaction of the *NCS2* QTL with the first major-effect QTL was background dependent, revealing a complex QTL architecture spanning these two linked loci. Such complex architecture suggests that more genes than can be predicted are likely to contribute to quantitative traits. The targeted backcrossing approach overcomes the difficulties posed by sample size, genetic linkage, and epistatic effects and facilitates identification of additional alleles with smaller contributions to complex traits.

THE identification of the responsible alleles for common, genetically complex phenotypes has remained difficult (Mackay 2001; Barton and Keightley 2002; Glazier *et al.* 2002; Botstein and Risch 2003; Flint *et al.* 2005). Difficulties arise from the lack of simple correspondence between phenotype and genotype caused by pleiotropy, genetic heterogeneity, gene–environment interactions, multifactorial inheritance, and epistasis. The study of complex traits has therefore benefited from understanding their genetic bases in model organisms (Steinmetz *et al.* 2002; Yalcin *et al.* 2004; Kroymann and Mitchell-Olds 2005; Mackay and Anholt 2006; Valdar *et al.* 2006; Keurentjes *et al.* 2007).

Yeast, *Saccharomyces cerevisiae*, is an informative model to dissect quantitative traits and several phenotypes have been investigated so far, including high-temperature growth (Htg) (Steinmetz *et al.* 2002; Sinha *et al.* 2006), sporulation (Deutschbauer and Davis 2005; Ben-Ari *et al.* 2006; Gerke *et al.* 2006), mRNA expression profiles (Brem *et al.* 2002, 2005; Yvert *et al.* 2003), small molecule sensitivities (Perlstein *et al.* 2007), cell morphology (Nogami *et al.* 2007), telomere length (Gatbonton *et al.* 2006), ethanol tolerance and growth (Hu *et al.* 2007; Smith and Kruglyak 2008), flocculation (Brauer *et al.* 2006), and physiological wine traits (Marullo *et al.* 2007). In addition, the full genome sequence of the laboratory strain, S288c (Goffeau *et al.* 1996), and of a few dozens of other strains (Wei *et al.* 2007, http://www.broad.mit.edu/annotation/genome/saccharomyces_cerevisiae/Info.html/ and http://www.sanger.ac.uk/Teams/Team71/durbin/sgrp/index.shtml) provide resources for complex trait dissection.

*S. cerevisiae* is an opportunistic pathogen (Enache-Angoulvant and Hennequin 2005) and the ability of clinical isolates to grow at high temperature facilitates their pathogenesis (McCusker *et al.* 1994). In a previous study of the Htg phenotype, we identified a 32-kb interval on chromosome XIV containing three Htg genes forming a QTL with a complex genetic architecture (Steinmetz *et al.* 2002). The three genes did not show an obvious role in Htg: *MKT1* encodes a protein involved in the post-transcriptional regulation of *HO* mRNA, *END3* encodes a gene product involved in endocytosis, actin cytoskeleton organization, and cell wall morphogenesis,

Sequence data from this article have been deposited with the GenBank Database under accession nos. EF125216–EF125228.

[1]*Present address:* Department of Biological Sciences, Tata Institute of Fundamental Research, Mumbai 400 005, India.

[2]These authors contributed equally to this work.

[3]*Corresponding author:* European Molecular Biology Laboratory, Meyerhofstrasse 1, 69117 Heidelberg, Germany. E-mail: larsms@embl.de

and *RHO2* encodes a small GTPase involved in establishment of cell polarity and in microtubule assembly. Moreover, common, rare, coding and noncoding polymorphisms were found to be causative, with alleles having additive and epistatic effects (Steinmetz *et al.* 2002; Sinha *et al.* 2006). Interactions between genes and strain background were detected as well, with the causative variants in these genes making background-dependent contributions to growth at high temperature (Sinha *et al.* 2006). These findings suggest a complex genetic architecture that might complicate the identification of additional QTL.

Several QTL mapping strategies have successfully identified major-effect loci on the basis of their strong association with the phenotype in segregating populations (Lander and Botstein 1989; Darvasi 1998; Brem *et al.* 2002; Wang *et al.* 2003; Flint *et al.* 2005; Keurentjes *et al.* 2007). Although mapping strategies have been designed to detect minor-effect loci (Darvasi 1998; Satagopan *et al.* 2007), many of these strategies have had poor success rates, due to the confounding effects of major loci and epistasis (Flint *et al.* 2005). In a recent study, a two-stage search strategy was used to first map the major-effect QTL and then to partition segregants on the basis of genotype at this locus: each subgroup of segregants (sharing one allele at the first QTL) was then used to map secondary loci that would not have been detected in single locus searches (Brem *et al.* 2005). Such two-step approaches, however, become impractical when the major-effect allele is present in most segregants, since the sample size of segregants lacking this allele may be too small for further QTL detection. To avoid the confounding effects of major loci, epistasis, and sample size, we used a targeted backcross mapping strategy that genetically eliminated the major effect of the previously identified QTL (Steinmetz *et al.* 2002). This strategy facilitated the mapping of three novel QTL contributing to Htg. The dissection of one novel QTL using reciprocal hemizygosity analysis (RHA) (Steinmetz *et al.* 2002) identified *NCS2* as the causative gene. Possible roles of *NCS2* in Htg were investigated by genomewide analyses of gene expression and by competitive growth of the pooled gene-deletion collection. A background-dependent interaction between *NCS2* and *MKT1* was found, which, along with the physical linkage between the two QTL, emphasizes the genetic complexity underlying quantitative traits.

## MATERIALS AND METHODS

**Strains, growth conditions, and RHA competitions:** Laboratory and clinically derived *S. cerevisiae* strains used in this work were isogenic derivatives of S288c and YJM421 (McCusker *et al.* 1994, supplemental Table S1). A naturally occurring *cox15* mutation in YJM421 (Ito-Harashima *et al.* 2002) was repaired to a functional *COX15* gene, as Cox15p function is needed for sporulation. Haploid derivatives of S288c and YJM421 were crossed and tetrads were dissected to generate meiotic segregants. Segregants were analyzed for Htg by colony size assay at 41°. For the targeted backcross mapping strategy, segregants were selected such that they were $Htg^+$ but contained the $Htg^-$ allele of the previously identified QTL and were then backcrossed to S288c. Strain manipulations and gene deletions were done using standard techniques (Rose *et al.* 1990; Wach *et al.* 1994; Goldstein and McCusker 1999; Sinha *et al.* 2006). Standard growth media and sporulation conditions were used as described previously (Rose *et al.* 1990; Sinha *et al.* 2006). Yeast strains were grown at 30°, unless otherwise stated.

All genes in the QTL interval were tested by RHA which was performed at 30° and 41°. Briefly, in RHA, equal numbers of cells of a hemizygote carrying only an S288c-derived allele of a gene and a hemizygote carrying only an YJM421-derived allele of the same gene, each marked with a different dominant drug-resistance marker, were combined and competed at high temperature. After 48-hr growth, the numbers of colony-forming units (CFU) of each strain were counted to determine growth phenotypes and thus, to identify the causative alleles in the QTL.

RHA competitions of pairs of reciprocally hemizygous hybrids and the reference hybrid (YJM421/S288c) strain assessed the contributions of individual alleles of *MKT1* or *NCS2*. To assess genetic interactions between *NCS2* and *MKT1*, competitions were performed between pairs of YJM421/S288c hybrid strains hemizygous for both *NCS2* and *MKT1* with the reference YJM421/S288c hybrid. All competitions were carried out in replicates using independently constructed strains. For RHA competitions, CFU $ml^{-1}$ counts of strains were normalized to the reference YJM421/S288c hybrid strain, all grown at 41° and tested for significance by Tukey–Kramer's honestly significant differences (HSD) test.

**Genotyping, linkage analysis, and DNA sequencing:** For the polymorphism scans, total genomic DNA was fragmented, labeled, and hybridized to Affymetrix yeast S98 arrays; biallelic markers were determined by the decreased hybridization efficiency of V1-09 (isogenic with YJM421) relative to S103 (isogenic with S288c), as described previously (Steinmetz *et al.* 2002). For linkage analysis, genomic DNA hybridization data were analyzed to determine the allele of every segregant at each marker by comparing the normalized probe intensity to the expected from the parental hybridizations. Regions were considered a QTL if segregation bias toward either one of the parental alleles was observed. Candidate QTL and their boundaries were further verified and fine-structure mapped by a segregation bias analysis using larger numbers of $Htg^+$ and random segregants, as well as several markers across the region. Individual markers were genotyped by denaturing high performance liquid chromatography (DHPLC) or, in a few cases, scored by fluorescence polarization genotyping (Kwok 2002) or direct sequencing. Dideoxy sequencing with big dye terminators was performed on ~600 bp PCR products tiled over intervals with at least ~50 bp overlaps. The Htg-QTL-2 sequences of all strains were submitted to GenBank (accession nos. EF125216–EF125228).

**Genomewide gene expression analysis:** Total RNA was isolated from wild-type and *ncs2*Δ S288c-background strains grown at 30° and processed for array hybridization (David *et al.* 2006). The resulting cDNA was hybridized to Affymetrix yeast S98 arrays and the hybridization data were analyzed using a DChip2006 package (Li and Wong 2001) to find genes with more than 1.5-fold expression difference. This cutoff was selected to find the genes that due to the loss of *NCS2* change their expression most and to reduce the chances of false positive calls.

**Deletion strains pool analysis:** The heterozygous deletion pool of essential genes (HetEss, containing ~1200 unique strains) and the homozygous deletion pool of nonessential

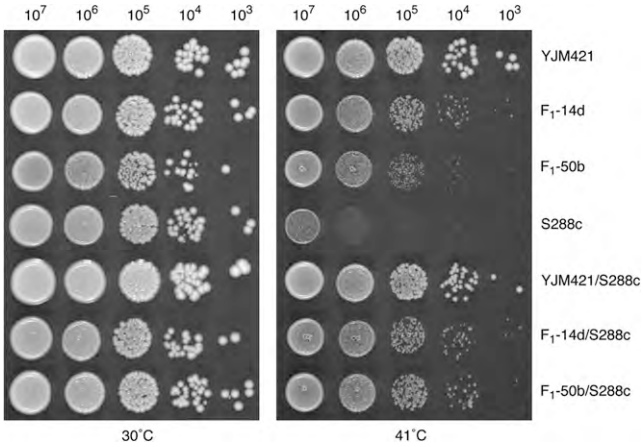


FIGURE 1.—Growth of the studied strains at high temperature. Spot dilutions showing growth at 30° and 41° of the YJM421/S288c background strains used to map Htg QTL. Tenfold dilutions were spotted on a YPD plate and incubated for 48 hr. All strains are diploids.

genes (HomDip, containing ~5000 unique strains) were analyzed for fitness differences of deletion strains at 30° and 37°. Sample preparation, array hybridizations, and data analysis were done as described (ST. ONGE *et al.* 2007). First, for each temperature, the average probe intensities from the final time point were compared against zero time point to calculate fold differences for each gene. Then, all the genes that showed a growth defect at 30° were excluded, to identify the genes with more than 1.5-fold difference in fitness between 30° and 37°.

**Construction of homologous *NCS2* SNP replacements:** Homologous *NCS2* SNP replacements were constructed in the haploid S288c background strain, YBN438, in which S288c-derived SNPs were replaced with YJM421-derived SNPs. For the *NCS2* coding SNP at position 212, a 50-bp region centered on position 212 was deleted and replaced with the *FCY1-NAT*MX4 cassette (SINHA *et al.* 2006). After introduction of an oligonucleotide containing the YJM421 SNP at position 212, 5-fluorocytosine-resistant transformants were selected, which were then screened for nourseothricin sensitivity. *NCS2* allele replacement transformants were confirmed by DNA sequencing. Desired transformants were crossed with *ncs2*Δ::Kan YJM421 background haploid strains to obtain hybrid strains with the genotype *NCS2-288(71L)/ncs2*Δ*::Kan*. These allele replacement hemizygous strains were competed with YJM421/S288c hemizygous hybrid strains containing only the YJM421-derived allele of *NCS2* and with the reference YJM421/S288c hybrid.

## RESULTS

**Mapping QTL using a targeted backcross strategy:** To identify a more complete spectrum of genes contributing to Htg, we used YJM421, a homozygous $Htg^+$ strain derived from a heterozygous clinical isolate found in the ascites fluid of a human patient (CLEMONS *et al.* 1994). YJM421 is genetically diverged from and grows better at high temperature than YJM145 (supplemental Figure S1A), the clinically derived strain used to identify Htg QTL in our previous study (STEINMETZ *et al.* 2002). Both YJM421 and the hybrid YJM421/S288c grow significantly better than S288c at 41° (Figure 1). A range of Htg phenotypes was observed when 600 haploid $F_1$ segregants of this hybrid were grown at 41°. Sixty-four segregants showed $Htg^+$ phenotypes similar to the $Htg^+$ parent by a colony-size assay. Under the assumption of independent segregation, at least three QTL affecting Htg were predicted ($64/600 = (1/2)^{3.23}$).

The first Htg QTL (Htg-QTL-1) was identified in the YJM145/S288c background and *MKT1* was the major-effect gene in that interval (STEINMETZ *et al.* 2002). Thus, we first tested if the linkage between *MKT1* and Htg also exists in the YJM421/S288c background. Among 64 $Htg^+$ $F_1$ segregants, 87.5% contained YJM421-derived alleles at this locus (Table 1, supplemental Figure S1B). This rate of inheritance suggested that several unlinked QTL, including *MKT1* itself, affect Htg also in the YJM421 background. Indeed, previous RHA results showed that the YJM421-derived allele of *MKT1* contributed to $Htg^+$ (SINHA *et al.* 2006). Thus, to uncover additional QTL, we tested an approach in which effects of previously known QTL are experimentally removed and targeted backcross progeny are used for mapping further QTL (Figure 2A).

Two haploid $F_1$ segregants ($F_1$-14d and $F_1$-50b) of the YJM421/S288c hybrid, which were $Htg^+$ but possessed S288c-derived alleles at Htg-QTL-1, were identified and backcrossed to S288c. Variation at Htg-QTL-1 was thus

**TABLE 1**

**Percentage of inheritance of YJM421-derived alleles in $Htg^+$ segregants of analyzed crosses**

| QTL (chromosome) | Coordinates (bp) (gene)[a] | YJM421/S288c ($F_1$) | $F_1$-14d/S288c ($BC_1$)[b] | $F_1$-50b/S288c ($BC_1$)[b] |
|---|---|---|---|---|
| Htg-QTL-1 (XIV) | 468,446 (*MKT1*) | 87.5 | NA[c] | NA[c] |
| Htg-QTL-2 (XIV) | 401,389 (*NCS2*) | 95.3 | 100.0 | NA[c] |
| Htg-QTL-3 (XV) | 948,437 | 73.4 | 77.5 | 92.3 |
| Htg-QTL-4 (IV) | 1,375,117 | 59.4[d] | 59.2[d] | 81.5 |

[a] Position of measured marker, relative to S288c sequence.
[b] $BC_1$, first generation of backcross.
[c] Not applicable (NA) since S288c-derived alleles were present at this position in both parental strains (see Figure 2B).
[d] Not significantly different from random segregation (50%).

fixed and, as a result, all segregants of the backcrosses had the Htg$^-$ S288c-derived allele at this locus. The two backcross diploids, $F_1$-14d/S288c and $F_1$-50b/S288c, were Htg$^+$, although less than the YJM421/S288c parental hybrid (Figure 1). This phenotypic difference was expected, as the backcross diploids lack the YJM421-derived Htg$^+$ allele of *MKT1* at Htg-QTL-1.

For mapping, we identified a set of 4191 evenly distributed biallelic single-feature polymorphism (SFP) markers between YJM421 and S288c, by hybridizing genomic DNA to high-density oligonucleotide microarrays (Winzeler *et al.* 1998). Independently, 656 and 820 haploid segregants from the $F_1$-14d/S288c and $F_1$-50b/S288c backcross diploids, respectively, were phenotyped for Htg by the colony-size assay. A range of Htg phenotypes was observed, of which 71 and 190 segregants had Htg$^+$ values as high as their Htg$^+$ haploid parents, $F_1$-14d and $F_1$-50b, respectively. On the basis of the phenotypic distribution, eliminating the effect of Htg-QTL-1 reduced the number of estimated unlinked QTL from 3.23 in $F_1$ segregants to 2.11 in the $F_1$-50b/S288c backcross segregants ($190/820 = (1/2)^{2.11}$). Surprisingly, in $F_1$-14d/S288c, the expectation stayed at 3.21 loci ($71/656 = (1/2)^{3.21}$), consistent with the slight Htg$^+$ advantage of $F_1$-14d over $F_1$-50b (Figure 1A).

Linkage analysis of 24 Htg$^+$ $F_1$-14d/S228c segregants identified two QTL on chromosomes XIV (Htg-QTL-2) and XV (Htg-QTL-3). Analysis of 21 Htg$^+$ $F_1$-50b/S228c segregants identified one QTL on chromosome IV (Htg-QTL-4) and a region on chromosome XV that overlaps Htg-QTL-3 (Figure 2B). In all three QTL, YJM421-derived alleles were linked with Htg$^+$. To fine map these QTL, 71 and 65 Htg$^+$ segregants of $F_1$-14d/S288c and $F_1$-50b/S288c, respectively, were genotyped by several SNP markers and the percentage of YJM421 inheritance was calculated across each interval (Figure 3). Htg-QTL-2, -3, and -4 were 15.0, 44.3, and 60.1 kb in size and contained 8, 16, and 28 ORFs, respectively (Table 2). All three QTL contained a large number of SNPs that changed coding sequences of the majority of corresponding ORFs (Table 2). Thus, the sequence variation between the parental strains was not a strong indicator of the responsible genes.

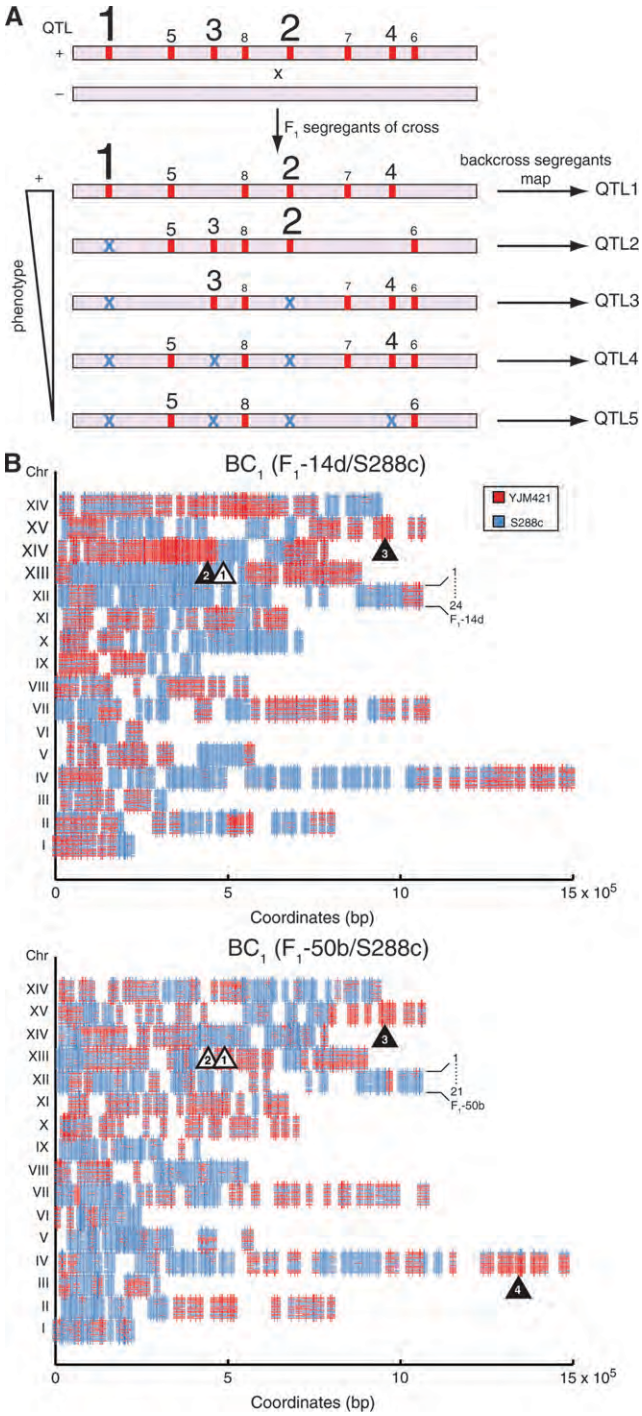


Figure 2.—(A) Targeted backcross mapping strategy to sequentially uncover QTL. Consider a quantitative trait in a (+) strain, defined by multiple QTL alleles (red bars) with different contributions to a phenotype (the larger the type size, the larger the phenotypic effect). $F_1$ segregants of a cross, between (+) and (−) parental stains, show a range of phenotypes. The best $F_1$ (+) segregant is backcrossed to the (−) parent. Analysis of these backcross segregants would fine map and identify QTL-1. Similar analysis of the next best $F_1$ (+) segregant that lacks QTL-1 (shown as blue ×) would then fine map QTL-2 in the next backcross segregants. Iterative fixation of major-effect QTL by a targeted selection of $F_1$ segregants for further backcrossing would map minor-effect QTL. (B) Genomic linkage scans of backcross segregants using microarrays. Genotypes of 24 and 21 backcross segregants of $F_1$-14d/S288c and $F_1$-50b/S288c, respectively, were determined by DNA hybridization. Vertical lines along chromosomes are SFPs; segregants are stacked by chromosome; YJM421-derived regions are in red, S288c-derived regions in blue. Htg QTL are marked with triangles (fixated ones indicated in white and newly detected in black). In $F_1$-14d/S288, Htg-QTL-1 (chromosome XIV) was fixed and Htg-QTL-2 (chromosome XIV) and Htg-QTL-3 (chromosome XV) were mapped. In $F_1$-50b/S288c, Htg-QTL-1 and Htg-QTL-2 (chromosome XIV) were fixed and Htg-QTL-3 (chromosome XV) and Htg-QTL-4 (chromosome IV) were mapped.

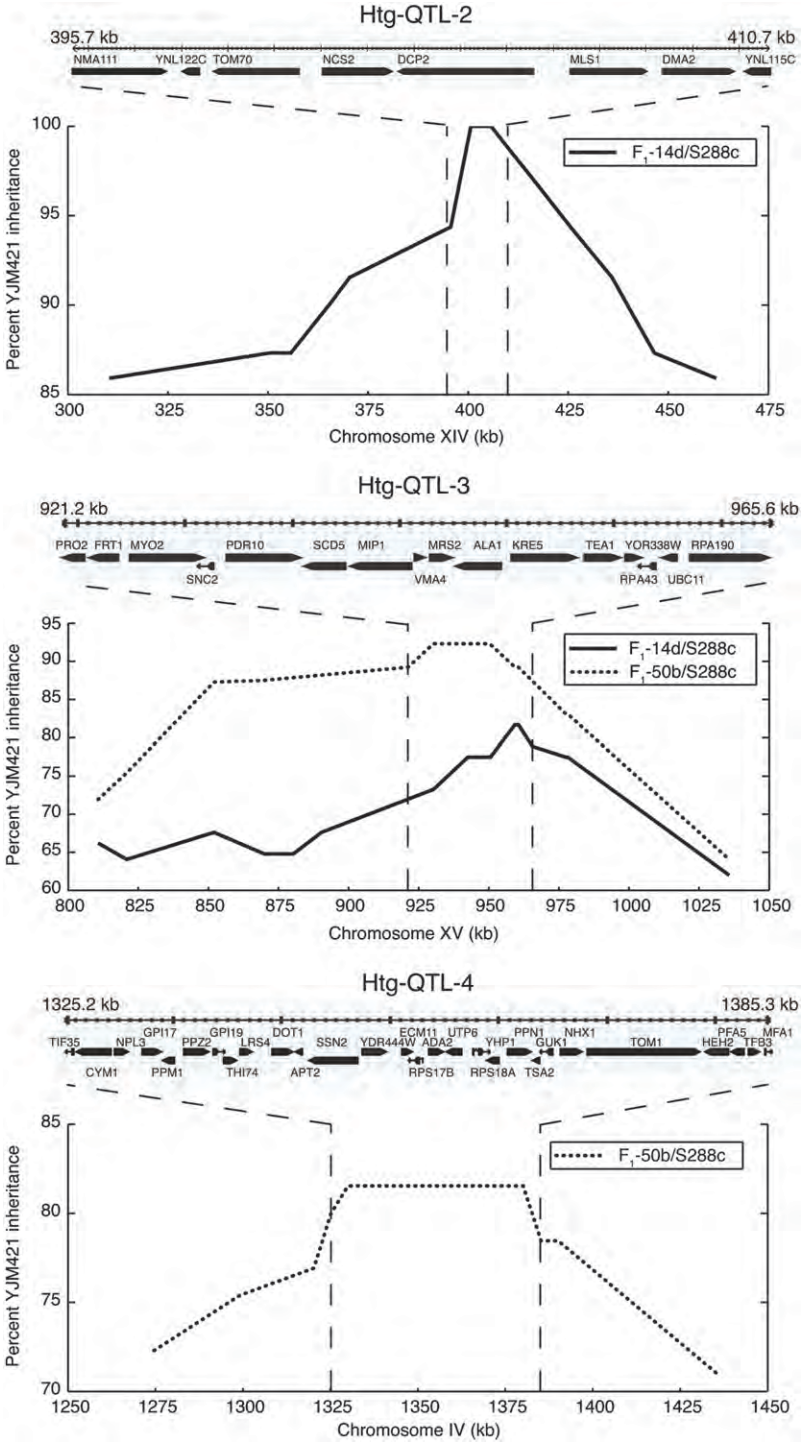


FIGURE 3.—Fine mapping of Htg QTL. Percentage of inheritance of YJM421-derived alleles among 71 and 65 $BC_1$ backcross segregants of $F_1$-14d/S288c and $F_1$-50b/S288c, respectively. For each QTL, boxes and names denote annotated genes.

To test for the effect of eliminating a major-effect allele on the degree of linkage of minor-effect loci, we compared the percentage of inheritance of YJM421-derived alleles between $Htg^+$ segregants of $F_1$ (YJM421/S288c) and that in each of the two backcross segregants ($F_1$-14d/S288c and $F_1$-50b/S288c). The segregants of $F_1$-14d/S288c backcross displayed a higher inheritance rate of YJM421-derived alleles at Htg-QTL-2 and -3 compared to $F_1$ segregants (Table 1). In addition, the absence of YJM421-derived alleles at two of four QTL in the $F_1$-50b/S288c backcross was accompanied by a more dramatic increase in the percentage of inheritance of YJM421-derived alleles at the remaining two QTL (Figure 3). These data suggest that the effect of a QTL can be concealed by the presence of other major-effect QTL.

**Identification of *NCS2* as the causative gene in Htg-QTL-2:** Our next step was to identify additional causative gene(s). Since the 100% $Htg^+$ linkage in the $F_1$-14d/S288c

**TABLE 2**

**Sequence analysis of Htg QTL**

| QTL (chromosome) | QTL coordinates[a] | Size (bp) | No. of genes[b] | Total SNPs[c] | No. of nonsynonymous SNPs | No. of genes with coding differences |
|---|---|---|---|---|---|---|
| Htg-QTL-2 (XIV) | 395,662–410,654 | 14,992 | 8 | 71 | 14 | 6 |
| Htg-QTL-3 (XV) | 921,238–965,555[d] | 44,317 | 16 | 84 | 22 | 10 |
| Htg-QTL-4 (IV) | 1,325,183–1,385,259[e] | 60,076 | 28 | 320 | 43 | 17 |

[a] Coordinates of the highest linkage peak relative to S288c sequence.
[b] Confirmed ORFs within QTL coordinates, according to SGD annotations (http://www.yeastgenome.org/).
[c] Sequence polymorphisms, including nucleotide substitutions, insertions and deletions, between YJM421 and S288c.
[d] Htg-QTL-3 coordinates are based on linkage data from $F_1$-14d/S288c and $F_1$-50b/S288c segregants (see Figure 3).
[e] Coordinates from 1,325,183–1,330,000 bp, 1,352,288–1,353,000 bp, and 1,384,924–1,385,259 bp relative to S288c sequence were not sequenced.

backcross suggested that Htg-QTL-2 on chromosome XIV had the strongest contribution, this QTL was chosen for further analysis.

First, we looked for potential association between polymorphisms and the trait. The entire Htg-QTL-2 interval was sequenced in six $Htg^+$ clinically derived strains and seven $Htg^-$ strains consisting of laboratory, wine, grape, and distillery strains. Four of the 238 sequence polymorphisms found among all sequenced strains exhibited slight marker-trait association ($P < 0.05$, $\chi^2$ test (not corrected for multiple testing); Figure 4). Notably, none of the 14 nonsynonymous SNPs between YJM421 and S288c was one of the associated four.

Second, since the genome of *S. cerevisiae* is well annotated, we attempted to use gene annotation to identify candidate Htg genes in Htg-QTL-2. However, the current annotation of gene function in Saccharomyces Genome Database (SGD) (http://www.yeastgenome.org/) gave no clear indication as to more likely causative genes.

Since association and annotation did not suggest candidate genes, we used RHA (Steinmetz *et al.* 2002) to functionally test the $Htg^+$ contribution of all eight annotated genes in Htg-QTL-2. In the YJM421/S288c hybrid background, no significant allele-specific growth differences were observed at 30° for any of the eight genes (data not shown). However, at 41°, replicate strains with the YJM421-derived allele of *NCS2* grew as well as the hybrid strain but better than strains with the S288c-derived allele, thus identifying *NCS2* as the causative gene (Figure 5).

**Identification of the causative SNP in *NCS2*:** *NCS2-421* has three synonymous and two nonsynonymous polymorphisms compared to the *NCS2-288* allele. Of the two nonsynonymous polymorphisms at positions 212 bp and 578 bp of the open reading frame, allele replacement analysis identified the A212T SNP, which creates a substitution at amino acid residue 71 from histidine in S288c to leucine in YJM421 (H71L), as the sole causative $Htg^+$ quantitative trait nucleotide (Figure 5). The effect of the nucleotide substitution as measured by RHA was identical to the full allele replacement, suggesting 71L was sufficient to confer the phenotype in the background of the hybrid.

The 212T allele is the common variant found in all isolates we sequenced, except S288c and its close relative W303 (Figure 4). Also, 19 of 32 other *S. cerevisiae* sequenced strains (Saccharomyces Genome Resequencing Project) and 6 species of the Saccharomyces family have this 212T allele.

**Functional analysis of *NCS2*:** *NCS2* encodes a protein with roles in urmylation as well as invasive and pseudohyphal growth (Goehring *et al.* 2003), none of which have obvious relevance to Htg. Therefore, to learn how *NCS2* might contribute to Htg, analyses of genomewide gene expression and pooled screening of the gene-deletion collection for growth defects at 37° were performed. Genomewide mRNA expression analysis between *ncs2* deletion and wild-type strains identified 371 differentially expressed genes (>1.5-fold, supplemental Table S2). Additionally, from the deletion pool screen, 989 genes were identified that when deleted resulted in a >1.5-fold difference in fitness at 37° compared to 30° (supplemental Table S3). Among the 56 genes common between the mRNA expression and gene-deletion pool data sets, we found enrichment for genes involved in tRNA and rRNA modification and in the ubiquitin pathway (Figure 6, supplemental Table S4). Our data, thus, are consistent with the predicted roles of Ncs2p in cell growth through post-transcriptional tRNA modification (Esberg *et al.* 2006), rRNA, and ribosome biosynthesis (Wade *et al.* 2006).

**Genetic interaction between *MKT1* and *NCS2*:** Several QTL studies in yeast (Brem *et al.* 2005; Deutschbauer and Davis 2005; Ben-Ari *et al.* 2006; Sinha *et al.* 2006) and other model organisms (Mackay 2004; Flint *et al.* 2005; Kroymann and Mitchell-Olds 2005) have shown both additive and epistatic relationships between QTL. We considered *NCS2* interactions with *END3*, *RHO2*, and *MKT1*, the three previously identified Htg genes (Steinmetz *et al.* 2002). For *END3*, S288c and YJM421 have the same causative SNP allele and thus no allele-specific contribution to Htg could be measured in the YJM421/S288c hybrid background (Sinha *et al.* 2006).

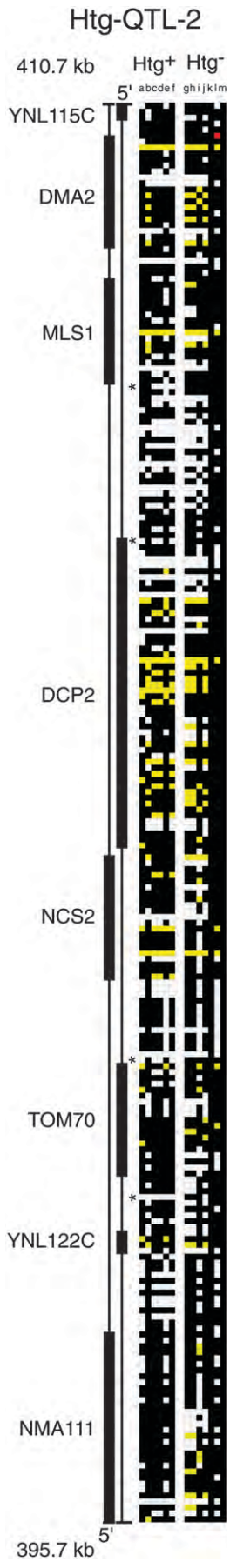


As the difference between *RHO2* hemizygotes was statistically nonsignificant, it was also excluded from further analysis.

In the YJM421/S288c background, at high temperature, the absence of the Htg$^+$ *NCS2-421* allele resulted in growth impairment similar to the absence of the Htg$^+$ *MKT1-421* allele. Strikingly, the absence of both *MKT1-421* and *NCS2-421* Htg$^+$ alleles resulted in growth impairment comparable to the loss of either single allele (Figure 5). That is, in the YJM421/S288c hybrid, the *MKT1-421* and *NCS2-421* Htg$^+$ alleles are epistatic: removal of either allele decreases Htg to an extent similar to removal of both alleles. This epistatic interaction in the hybrid is interesting when considering the segregation of both genes in the cross of the parental backgrounds. In the backcross hybrid, $F_1$-14d/S288c, *NCS2-421* is a contributor to Htg despite the strain being homozygous for the Htg$^-$ *MKT1-288* allele. Therefore, *NCS2* makes a contribution to Htg independent of *MKT1* in this $F_1$ background. Thus, the nature of the interaction between *NCS2* and *MKT1* is genetic background dependent.

The genetic interaction between *MKT1* and *NCS2* is furthermore striking given the close proximity of the two genes in the genome. The physical distance between *NCS2* and *MKT1* is 64.6 kb, translating to a genetic distance of 23 cM in random $F_1$ segregants. Remarkably, 86% of the 64 Htg$^+$ $F_1$ progeny contained Htg$^+$ alleles at both loci, supporting that these two alleles cosegregate as a linked locus (Figure 7). Thus, linkage between the genes and their epistatic interaction suggest that inheriting both Htg$^+$ alleles is advantageous for the phenotype.

## DISCUSSION

Increasingly, studies are indicating that QTL architectures are complex, containing blocks of linked loci of various effect sizes (Brem and Kruglyak 2005; Kroymann and Mitchell-Olds 2005; Mackay and Anholt 2006; Valdar *et al.* 2006). These complexities render dissecting polygenic QTL a challenge. While $F_1$ and $F_2$ families are quicker to obtain and require more progeny to map moderate effect QTL, backcross and backcross-derived strategies (Darvasi 1998; Hospital

Figure 4.—Sequence variation analysis of the Htg-QTL-2 (chromosome XIV; 395,662–410,654 bp) among six Htg$^+$ and seven Htg$^-$ yeast strains. Each column represents a strain and each row a sequence variant relative to S288c (black). White are synonymous and yellow are nonsynonymous variants. Variants with significant marker-trait association are marked (*). Rows (a–f) show Htg$^+$ strains: YJM421 (a), YJM326 (b), YJM320 (c), YJM280 (d), YJM339 (e), and YJM789 (f). Rows (g–m) show Htg$^-$ strains: YJM270 (g), YJM269 (h), YJM627 (i), YJM1129 (j), W303 (k), SK1 (l), and S288c (m).

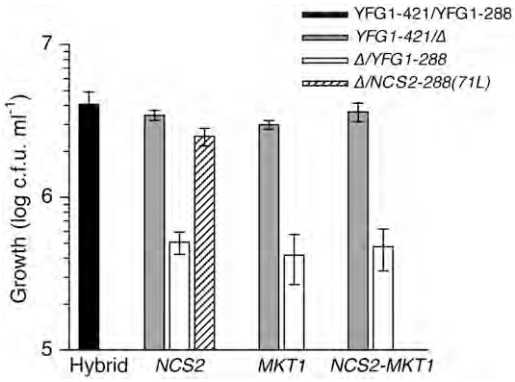


FIGURE 5.—RHA analysis of *NCS2*, *MKT1*, *NCS2-MKT1*, and *NCS2-288(71L)*. Solid bar denotes the hybrid strain, XHS740, used as reference and for comparison in each competition. Shaded bars denote hemizygous hybrid strains containing the YJM421-derived allele(s) while open bars denote those that contain the S288c-derived allele(s). The striped bar denotes the hemizygous hybrid strain containing the 71L $Htg^+$ SNP allele of YJM421 inside the otherwise S288c-derived allele of *NCS2*. All assays were carried out in the diploid hybrid background (YJM421/S288c) at 41°. For each gene, three independent measurements were taken and averaged after normalization between replicates and genes using a reference hybrid strain. All *NCS2-421*/Δ, *MKT1-421*/Δ, and Δ/*NCS2-288(71L)* hybrids grow similar to each other but significantly better than the hemizygotes with S288c-derived alleles (Tukey–Kramer HSD test, $P < 0.05$).

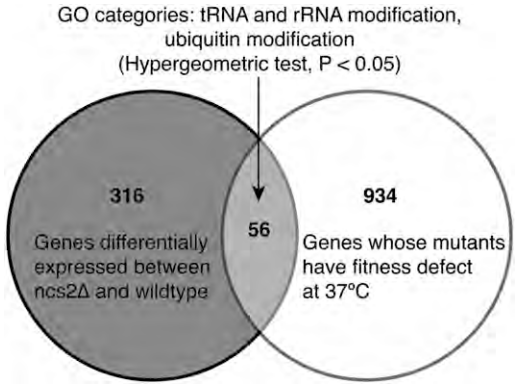


FIGURE 6.—Functional analysis of *NCS2*. Overlap in gene lists between genes differentially expressed (>1.5-fold) in *ncs2* deletion strain and genes that when deleted cause a fitness defect at 37°. GO category enrichments are indicated for the genes common between the two data sets.

2005) increase mapping chances by isolating individual QTL and narrowing down the linked intervals. Such QTL dissection has typically required extensive genotyping and advanced generations of segregating progeny. Here, using targeted backcross mapping to fix the effects of previously identified QTL, we efficiently identified new QTL with minor effects and resolved a polygenic QTL into component quantitative trait genes. This was possible by genomewide genotyping of only a few $BC_1$ segregants due to increased linkage of minor loci with the phenotype upon eliminating the masking effect of a major QTL. The fact that minor alleles are more readily detected supports the usefulness and efficiency of the targeted backcross mapping strategy.

Both polygenic QTL and epistatic interactions among QTL contribute to the complex genetic architecture of quantitative traits (*e.g.*, ESHED and ZAMIR 1996; CORDELL 2002; CARLBORG and HALEY 2004; BADANO *et al.* 2006; SINHA *et al.* 2006). So far, the genetic basis of Htg in clinical isolates includes four physically linked genes (*MKT1*, *END3*, *RHO2*, and *NCS2*), which show background-dependent contributions and interactions. Two more QTL were identified on other chromosomes. Multiple QTL, physical linkage, background specific epistasis, and varying allele contributions suggest that a larger number of genes are likely to contribute to this and other quantitative traits than can be predicted. Identifying most genes of a quantitative trait requires additional mapping strategies, like targeted backcrossing, which differ in their sensitivity to such confounding genetic relationships and can be carried out also in organisms other than yeast. The detection of milder-effect QTL provides a step toward a comprehensive list of genes contributing to quantitative traits and thus is a necessary requirement to a complete understanding of the relationship between DNA sequence and phenotypic variation.

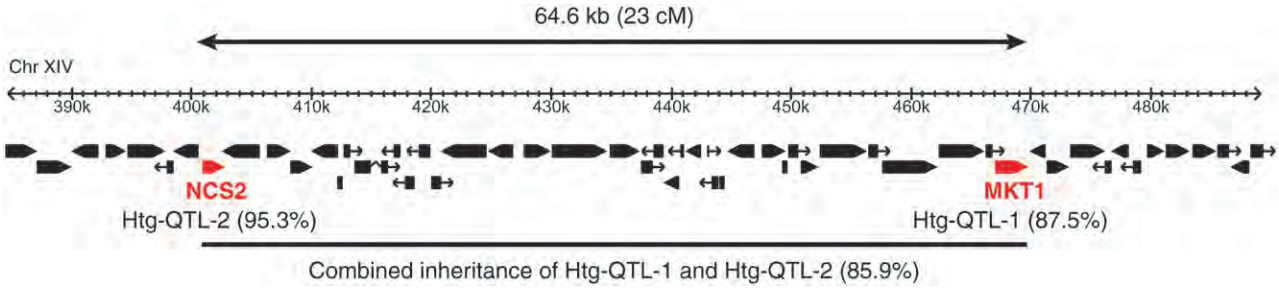


FIGURE 7.—Architecture of the chromosome XIV $Htg^+$ complex QTL. *MKT1* (Htg-QTL-1) and *NCS2* (Htg-QTL-2), shown in red, are two linked Htg genes on chromosome XIV. Boxes denote annotated genes. On top, physical and genetic distance between the QTL alleles is shown, as calculated from random $F_1$ segregants of the YJM421/S288c background. Along with the QTL names, the percentage of association of each $Htg^+$ QTL individually is indicated (see Table 1). The combined inheritance of the linked QTL among $Htg^+$ $F_1$ segregants in the YJM421/S288c background is shown at the bottom.

We would like to thank G. Ben-Ari for experimental contributions. This research was supported by grants from Israeli Science Foundation (L.D.), BayGene (P.J.O.), National Institutes of Health (J.H.M. and L.M.S.), and Deutsche Forschungsgemeinschaft (L.M.S.).

## LITERATURE CITED

Badano, J. L., C. C. Leitch, S. J. Ansley, H. May-Simera, S. Lawson *et al.*, 2006 Dissection of epistasis in oligogenic Bardet-Biedl syndrome. Nature **439:** 326–330.

Barton, N. H., and P. D. Keightley, 2002 Understanding quantitative genetic variation. Nat. Rev. Genet. **3:** 11–21.

Ben-Ari, G., D. Zenvirth, A. Sherman, L. David, M. Klutstein *et al.*, 2006 Four linked genes participate in controlling sporulation efficiency in budding yeast. PLoS Genet. **2:** e195.

Botstein, D., and N. Risch, 2003 Discovering genotypes underlying human phenotypes: past successes for Mendelian disease, future approaches for complex disease. Nat. Genet. **33**(Suppl): 228–237.

Brauer, M. J., C. M. Christianson, D. A. Pai and M. J. Dunham, 2006 Mapping novel traits by array-assisted bulk segregant analysis in *Saccharomyces cerevisiae*. Genetics **173:** 1813–1816.

Brem, R. B., and L. Kruglyak, 2005 The landscape of genetic complexity across 5,700 gene expression traits in yeast. Proc. Natl. Acad. Sci. USA **102:** 1572–1577.

Brem, R. B., G. Yvert, R. Clinton and L. Kruglyak, 2002 Genetic dissection of transcriptional regulation in budding yeast. Science **296:** 752–755.

Brem, R. B., J. D. Storey, J. Whittle and L. Kruglyak, 2005 Genetic interactions between polymorphisms that affect gene expression in yeast. Nature **436:** 701–703.

Carlborg, O., and C. S. Haley, 2004 Epistasis: Too often neglected in complex trait studies? Nat. Rev. Genet. **5:** 618.

Clemons, K. V., J. H. McCusker, R. W. Davis and D. A. Stevens, 1994 Comparative pathogenesis of clinical and nonclinical isolates of *Saccharomyces cerevisiae*. J. Infect. Dis. **169:** 859–867.

Cordell, H. J., 2002 Epistasis: what it means, what it doesn't mean, and statistical methods to detect it in humans. Hum. Mol. Genet. **11:** 2463–2468.

Darvasi, A., 1998 Experimental strategies for the genetic dissection of complex traits in animal models. Nat. Genet. **18:** 19–24.

David, L., W. Huber, M. Granovskaia, J. Toedling, C. J. Palm *et al.*, 2006 A high-resolution map of transcription in the yeast genome. Proc. Natl. Acad. Sci. USA **103:** 5320–5325.

Deutschbauer, A. M., and R. W. Davis, 2005 Quantitative trait loci mapped to single-nucleotide resolution in yeast. Nat. Genet. **37:** 1333–1340.

Enache-Angoulvant, A., and C. Hennequin, 2005 Invasive Saccharomyces infection: a comprehensive review. Clin. Infect. Dis. **41:** 1559–1568.

Esberg, A., B. Huang, M. J. Johansson and A. S. Bystrom, 2006 Elevated levels of two tRNA species bypass the requirement for elongator complex in transcription and exocytosis. Mol. Cell **24:** 139–148.

Eshed, Y., and D. Zamir, 1996 Less-than-additive epistatic interactions of quantitative trait loci in tomato. Genetics **143:** 1807–1817.

Flint, J., W. Valdar, S. Shifman and R. Mott, 2005 Strategies for mapping and cloning quantitative trait genes in rodents. Nat. Rev. Genet. **6:** 271–286.

Gatbonton, T., M. Imbesi, M. Nelson, J. M. Akey, D. M. Ruderfer *et al.*, 2006 Telomere length as a quantitative trait: genome-wide survey and genetic mapping of telomere length-control genes in yeast. PLoS Genet. **2:** e35.

Gerke, J. P., C. T. Chen and B. A. Cohen, 2006 Natural isolates of *Saccharomyces cerevisiae* display complex genetic variation in sporulation efficiency. Genetics **174:** 985–997.

Glazier, A. M., J. H. Nadeau and T. J. Aitman, 2002 Finding genes that underlie complex traits. Science **298:** 2345–2349.

Goehring, A. S., D. M. Rivers and G. F. Sprague, Jr., 2003 Urmylation: a ubiquitin-like pathway that functions during invasive growth and budding in yeast. Mol. Biol. Cell **14:** 4329–4341.

Goffeau, A., B. G. Barrell, H. Bussey, R. W. Davis, B. Dujon *et al.*, 1996 Life with 6000 genes. Science **274:** 546, 563–567.

Goldstein, A. L., and J. H. McCusker, 1999 Three new dominant drug resistance cassettes for gene disruption in *Saccharomyces cerevisiae*. Yeast **15:** 1541–1553.

Hospital, F., 2005 Selection in backcross programmes. Philos. Trans. R. Soc. Lond. B Biol. Sci. **360:** 1503–1511.

Hu, X. H., M. H. Wang, T. Tan, J. R. Li, H. Yang *et al.*, 2007 Genetic dissection of ethanol tolerance in the budding yeast *Saccharomyces cerevisiae*. Genetics **175:** 1479–1487.

Ito-Harashima, S., P. E. Hartzog, H. Sinha and J. H. McCusker, 2002 The *tRNA-Tyr* gene family of *Saccharomyces cerevisiae*: agents of phenotypic variation and position effects on mutation frequency. Genetics **161:** 1395–1410.

Keurentjes, J. J., L. Bentsink, C. Alonso-Blanco, C. J. Hanhart, H. Blankestijn-De Vries *et al.*, 2007 Development of a near-isogenic line population of *Arabidopsis thaliana* and comparison of mapping power with a recombinant inbred line population. Genetics **175:** 891–905.

Kroymann, J., and T. Mitchell-Olds, 2005 Epistasis and balanced polymorphism influencing complex trait variation. Nature **435:** 95–98.

Kwok, P. Y., 2002 SNP genotyping with fluorescence polarization detection. Hum. Mutat. **19:** 315–323.

Lander, E. S., and D. Botstein, 1989 Mapping Mendelian factors underlying quantitative traits using RFLP linkage maps. Genetics **121:** 185–199.

Li, C., and W. H. Wong, 2001 Model-based analysis of oligonucleotide arrays: expression index computation and outlier detection. Proc. Natl. Acad. Sci. USA **98:** 31–36.

Mackay, T. F., 2001 Quantitative trait loci in Drosophila. Nat. Rev. Genet. **2:** 11–20.

Mackay, T. F., 2004 The genetic architecture of quantitative traits: lessons from Drosophila. Curr. Opin. Genet. Dev. **14:** 253–257.

Mackay, T. F., and R. R. Anholt, 2006 Of flies and man: Drosophila as a model for human complex traits. Annu. Rev. Genomics Hum. Genet. **7:** 339–367.

Marullo, P., M. Aigle, M. Bely, I. Masneuf-Pomarede, P. Durrens *et al.*, 2007 Single QTL mapping and nucleotide-level resolution of a physiologic trait in wine *Saccharomyces cerevisiae* strains. FEMS Yeast Res. **7:** 941–952.

McCusker, J. H., K. V. Clemons, D. A. Stevens and R. W. Davis, 1994 Genetic characterization of pathogenic *Saccharomyces cerevisiae* isolates. Genetics **136:** 1261–1269.

Nogami, S., Y. Ohya and G. Yvert, 2007 Genetic complexity and quantitative trait loci mapping of yeast morphological traits. PLoS Genet. **3:** e31.

Perlstein, E. O., D. M. Ruderfer, D. C. Roberts, S. L. Schreiber and L. Kruglyak, 2007 Genetic basis of individual differences in the response to small-molecule drugs in yeast. Nat. Genet. **39:** 496–502.

Rose, M. D., F. Winston and P. Hieter, 1990 *Methods in Yeast Genetics: A Laboratory Course Manual*. Cold Spring Harbor Laboratory Press, Cold Spring Harbor, NY.

Satagopan, J. M., S. Sen and G. A. Churchill, 2007 Sequential quantitative trait locus mapping in experimental crosses. Stat. Appl. Genet. Mol. Biol. **6:** Article 12.

Sinha, H., B. P. Nicholson, L. M. Steinmetz and J. H. McCusker, 2006 Complex genetic interactions in a quantitative trait locus. PLoS Genet. **2:** e13.

Smith, E. N., and L. Kruglyak, 2008 Gene-environment interaction in yeast gene expression. PLoS Biol. **6:** e83.

St. Onge, R. P., R. Mani, J. Oh, M. Proctor, E. Fung *et al.*, 2007 Systematic pathway analysis using high-resolution fitness profiling of combinatorial gene deletions. Nat. Genet. **39:** 199.

Steinmetz, L. M., H. Sinha, D. R. Richards, J. I. Spiegelman, P. J. Oefner *et al.*, 2002 Dissecting the architecture of a quantitative trait locus in yeast. Nature **416:** 326–330.

Valdar, W., L. C. Solberg, D. Gauguier, S. Burnett, P. Klenerman *et al.*, 2006 Genome-wide genetic association of complex traits in heterogeneous stock mice. Nat. Genet. **38:** 879–887.

Wach, A., A. Brachat, R. Pohlmann and P. Philippsen, 1994 New heterologous modules for classical or PCR-based gene disruptions in *Saccharomyces cerevisiae*. Yeast **10:** 1793–1808.

Wade, C. H., M. A. Umbarger and M. A. McAlear, 2006 The budding yeast rRNA and ribosome biosynthesis (RRB) regulon contains over 200 genes. Yeast **23:** 293–306.

Wang, X., I. Le Roy, E. Nicodeme, R. Li, R. Wagner *et al.*, 2003 Using advanced intercross lines for high-resolution mapping of HDL cholesterol quantitative trait loci. Genome Res. **13:** 1654–1664.

Wei, W., J. H. McCusker, R. W. Hyman, T. Jones, Y. Ning *et al.*, 2007 Genome sequencing and comparative analysis of *Saccharomyces cerevisiae* strain YJM789. Proc. Natl. Acad. Sci. USA **104:** 12825–12830.

Winzeler, E. A., D. R. Richards, A. R. Conway, A. L. Goldstein, S. Kalman *et al.*, 1998 Direct allelic variation scanning of the yeast genome. Science **281:** 1194–1197.

Yalcin, B., S. A. Willis-Owen, J. Fullerton, A. Meesaq, R. M. Deacon *et al.*, 2004 Genetic dissection of a behavioral quantitative trait locus shows that *Rgs2* modulates anxiety in mice. Nat. Genet. **36:** 1197–1202.

Yvert, G., R. B. Brem, J. Whittle, J. M. Akey, E. Foss *et al.*, 2003 Trans-acting regulatory variation in *Saccharomyces cerevisiae* and the role of transcription factors. Nat. Genet. **35:** 57–64.

Communicating editor: M. Johnston